ARMA 12-186

Numerical modeling of strain transfer from rock mass to a fibre optic sensor installed inside a grouted borehole

Madjdabadi, B. M.
Civil Engineering Department, University of Waterloo, Waterloo, Ontario, Canada
Benoît Valley
Geomechanics Research Centre, MIRARCO – Mining Innovation, Sudbury, Ontario, Canada
Maurice B. Dusseault
Earth and Environmental Sciences Department, University of Waterloo, Waterloo, Ontario, Canada
Peter K. Kaiser
CEMI, Sudbury, Ontario, Canada

This paper was prepared for presentation at the 46th US Rock Mechanics / Geomechanics Symposium held in Chicago, IL, USA, 24-27 June 2012.

ABSTRACT: Strain measurements in underground excavation are usually done locally, with extensometers or similar devices placed within 10-15 meters of adit or stope faces, mainly to gage development of the EDZ (excavation damaged zone) and assess its evolution and impact on local safety (rock falls, rapid deterioration of wall condition...). However, the calibration of three-dimensional stress analysis models used to assess excavation geometry and sequencing requires strain (displacement) measurements in those parts of the rock mass that are in the elastic domain for some or all of their active design life. Recently developed distributed fibre optic sensors are now being used to measure local linear displacements continuously in a large rock mass volume in real mining conditions in Canada. Grouted inside a borehole and therefore encased in a material of far lower stiffness that the rock mass, an optical fibre may register strains different from those actually occurring in the rock mass. A number of factors affect the process of rock mass strain conveyance through the grout to the fibre. This paper reports a study that simulates the borehole-grout-fibre interaction to find how the strain transfer takes place and whether there are any issues serious enough to warrant alterations in installation procedures and grout materials.

Keywords: strain measurement, fibre optic sensor, numerical modeling, rock mass stiffness, grout

1. INTRODUCTION

With depletion of shallow ore resources, extraction from deeper deposits becomes more and more justifiable in terms of costs. Working conditions in deep environments differ significantly, imposing more complexity as stresses are much higher. Any perturbations to previously balanced stress fields due to mining activities could result in severe damage and impairment of the safety of excavations.

Most attention has been paid to local characteristics of rock mass and support requirements when mining. However, deep mining with complex geometry involves much larger rock volumes, influencing stress and strain fields at a scale greater than a stope or other excavation. Stress perturbations lead to loading or unloading of pre-existing geological features such as faults and dikes which might already be in a critical state.

Far from opening boundaries, the rock mass deforms elastically because of strain propagation resulting from mining. Rock mass monitoring at distances beyond the excavation damaged and disturbed zones (EDZ) must be considered in design of each deep mining work to achieve σ-ε model calibration and improve predictions. Conventionally strain is measured at one point using devices like vibrating wire strain gauges, perhaps mounted on rockbolts at some distance from each other in a distributed manner to understand the deformation profile along a rockbolt installed close to the opening (in the EDZ) [1]. Recently developed fibre optic sensors permit use of a long optical fibre as a fully distributed strain sensor with a capability to measure strain with high spatial resolution over a substantial length.

Grouting such a fibre into a borehole remote from the EDZ is a promising approach for far-field deformation monitoring. However, a question arises as to exactly what the fibre senses when the rock mass is strained, whether the rock mass is massive or jointed. This paper studies parameters influencing the amount of strain transferred from rock mass to the optical fibre through

the grout. It also considers fibre mechanical behavior in the presence of fractures crossing the borehole.

2. CONTINUUM OR DISCONTINUUM…

When a body of rock is loaded, it experiences displacement in three modes: translation, rotation and strain [2]. Strain is defined by the displacement of adjacent points in the body relative to each other [3].

Rock masses are usually non-homogeneous and anisotropic: properties vary from point-to-point and with direction. Geological features such as joints, faults and fractures have a great effect on behavior. When a rock mass is disturbed, the density, nature and orientation of fractures with respect to the underground structure affect the rock mass deformation behavior, including the intact rock blocks and the discontinuities themselves.

A massive rock mass is expected to deform uniformly when it is loaded by a constant and uniformly distributed stress. As shown in Fig. 1a, a 2D square-shaped body of a rock that is uniformly stresses experiences homogeneous strain, giving a new rectangular shape. Accumulated displacement over the central dashed line would be as shown in Fig. 1b. Since the body of rock is homogeneous, displacement will linearly vary and strain along this length is constant.

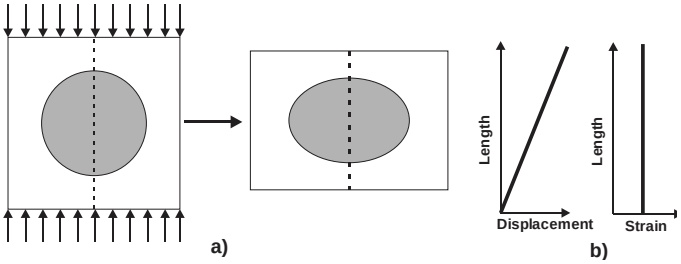

Fig. 1. a) Deformed homogenous rock body, b) strain and displacement changes over dashed line

However, when the rock mass is jointed, it may be viewed as assemblage of smaller blocks; its behavior is now quite different as the fractures play an important role as the mass is stressed. It is schematically shown in Fig. 2a how the same body of rock in Fig. 1 containing two perpendicular joint sets might react to an initially uniform stress. Most of the deformation along the dashed line in Fig. 2a happens where it intersects a fracture. Strain in the rock blocks is usually small compared to fracture slippage, so much so that block strains are usually ignored ("rigid block" model). This is more the case when the number of joint sets is limited and rock blocks are sensibly treated as rigid, but if the rock mass is heavily jointed, it behaves more as an "equivalent continuum" with modified mechanical properties.

To assess the displacement field in the rock mass, it is necessary to interpret the linear strain measurements taken along a borehole in the rock mass using the fibre optic sensor (FOS) cable grouted into the borehole. Because the FOS monitoring data shows what the fibre senses, the size of borehole and grout properties may be influential in interpreting the process of strain transfer from the rock mass to the fibre. In the following sections a series of numerical models is presented to simulate the effects of the grout and borehole on this process.

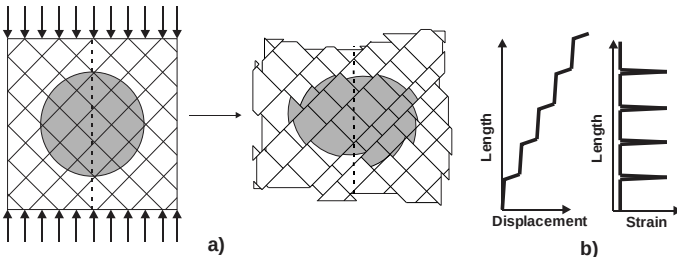

Fig. 2. a) Deformation of a rock mass, b) strain and displacement changes over dashed line

Also of importance is the case when strain localization occurs where a fracture traverses the borehole. Since in hard rock mining the borehole grout is commonly much softer than surrounding rock mass, it is expected that slippage of the grout creates a deformation band rather than generating a sharp break, as in the rock mass. Fig. 3 shows two possible cases. When grout is extremely stiff a brittle break through it is developed with a deformation bandwidth (w) approaching zero (Fig. 3a) inducing a locally infinite extension to the fibre (i.e. breakage). In the other case (Fig. 3b), the width of the deformation band is larger than zero and involves a length of the fibre during its extension where fibre sections above and below the slip region are offset (o) in the slip direction. Hence, the maximum elongation of fibre, before breakage happens, is essential to consider during shear deformation interpretation within the rock mass.

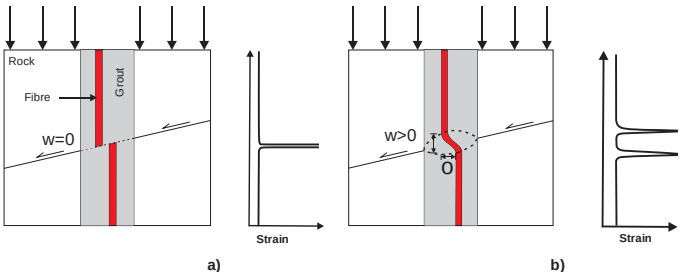

Fig. 3. a) Brittle failure of grout and fibre as fracture slips, b) deformation band creation with fracture movement

3. NUMERICAL MODELLING

The two-dimensional, plane strain, elasto-plastic finite element code Phase2 (RocScience, 2012) was used to simulate the rock/grout/fiber system. The model developed was 1×1 m in size (see Fig. 4) and was cut by a grout-filled, 10 cm hole and a 8 mm fiber optic cable through its vertical axis. Because of the plane strain conditions, the borehole was actually approximated by a slot. Almost 50000 3-noded triangular meshes with sizes ranging from 2-10 mm were created. Zero initial stress

conditions were chosen, then the loading was applied. The boundary conditions were as following: zero-displacement (pinned) was imposed to the lower boundary, a 1 MPa constant stress was applied to the lateral boundaries and step-wise increasing displacement was enforced at the top boundary. Two 2-cm-deep notches at the top and bottom of the block were included to avoid applying any direct load on the grout and fibre. The displacement applied at the top boundary was increased from an initial value of 11.5 μm to a final value of 1.15 mm over 8 steps, factoring successively the initial value by 2, 3, 4, 5, 10, 20, 50 and 100. The initial 11.5 μm was chosen since it created almost 1 MPa stress in the model and large sequential factors were chosen to create high stress to see how the fibre strain registration varied. Three model cases were considered: an homogeneous rock, a rock with a single 80 cm long joint, and a rock mass with two joint sets. In the latter case, the lateral boundary conditions selected were zero displacement instead of constant stress. Table 1 summarizes material and joint properties for various models. Two cross-sectional profiles, one in the rock and one at the fibre, were considered to measure vertical strain along their length (dashed lines in Fig. 4). The location for the profile in the rock was examined so that over the height of the block the strain was consistent.

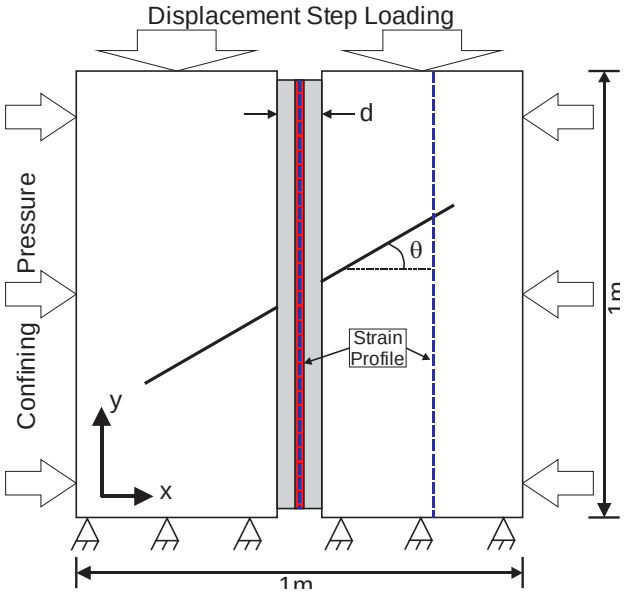

Fig. 4. Model Geometry and boundary condition in Phase 2

Table 1. Material and joint properties

Properties	Rock	Grout	Fibre	Joint
Density (kg/m^3)	2700	2100	688	-
Young's Modulus (GPa)	88	16	0.44	-
Poisson's Ratio	0.11	0.18	0.25	-
Cohesion (MPa)	71	15	-	0
Friction Angle	48	22	-	25
Tensile Strength (MPa)	11	0.01	-	0
Normal Stiffness (GPa/m)	-	-	-	250
Shear Stiffness (GPa/m)	-	-	-	100

CONTINUUM MODELLING

In this study it was assumed that the bonding efficiency at the rock-grout and grout-fibre boundary is perfect. An index called strain transfer rate (ST) can be defined as follows:

$$ST = \frac{\varepsilon_{l_{fibre}}}{\varepsilon_{l_{rock}}} \quad (1)$$

Here, ε_{lfibre} and ε_{lrock} are linear strains over the vertical profile in the fibre and rock, respectively, with compressional strain positive, extensional strain negative. Positive ST implies that both the fibre and rock experience the same strain type, while negative *ST* indicates opposite strain type. Sensitivity analyses were performed on the effect of step loading, grout stiffness, borehole size, and confining stress on the strain sensing response of the fibre. Fig. 5 shows a vertical stress contour at the 9th step (assuming elastic response). It is clear that the grout and fibre carry far less stress than the rock, even at higher loadings, because of the stiffness contrast and loading direction with respect to the borehole angle. It is found that grout and fibre at both ends of borehole experience tensile stress because of lack of confinement.

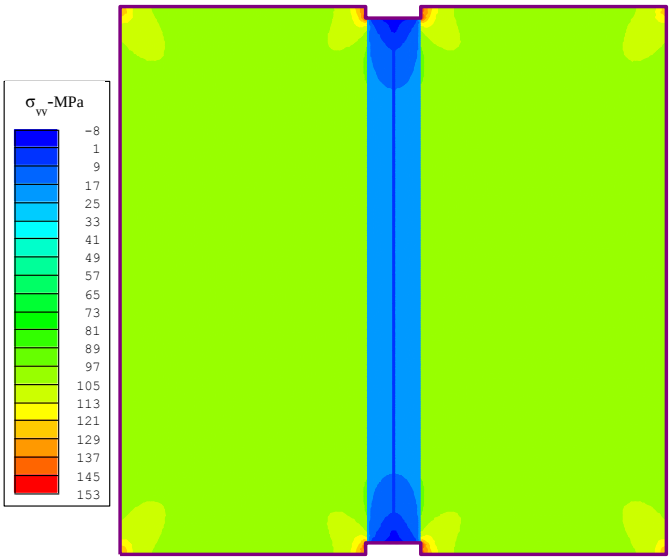

Fig. 5. Contour of vertical stress for elastic model at 9th step

Fig. 6a shows *ST* at selected displacement step loading for an elastic response of the rock and grout. At both ends of the borehole (0-0.1 & 0.9-1m) the fibre shows drastically different strain from the rock, so that it even undergoes extension (1). Moving away from the ends, the fibre's strain quickly approaches that in the rock. A concave-shaped strain profile (2) at low loadings transforms to an almost flat (3) profile as loadings increases so that at most of the fibre length strain is almost the same as the rock. Continuing loading to higher levels causes the fibre to register slightly different strain, creating a convex-shaped profile (4). Fig 6b

illustrates vertical to horizontal stress ratio (S_{yy}:S_{xx}) over the length of the fibre. It can be seen that the vertical stress is generally lower than the horizontal one due to lateral deformation of grout imposing stress on the fibre. It also can be seen that S_{yy}:S_{xx} follows almost the same trend that Fig 6a shows. For instance, at step 9 the strain profile from the middle of the fibre towards the ends shows a lower value (Fig. 6a) as it is less vertically stressed (Fig 6b).

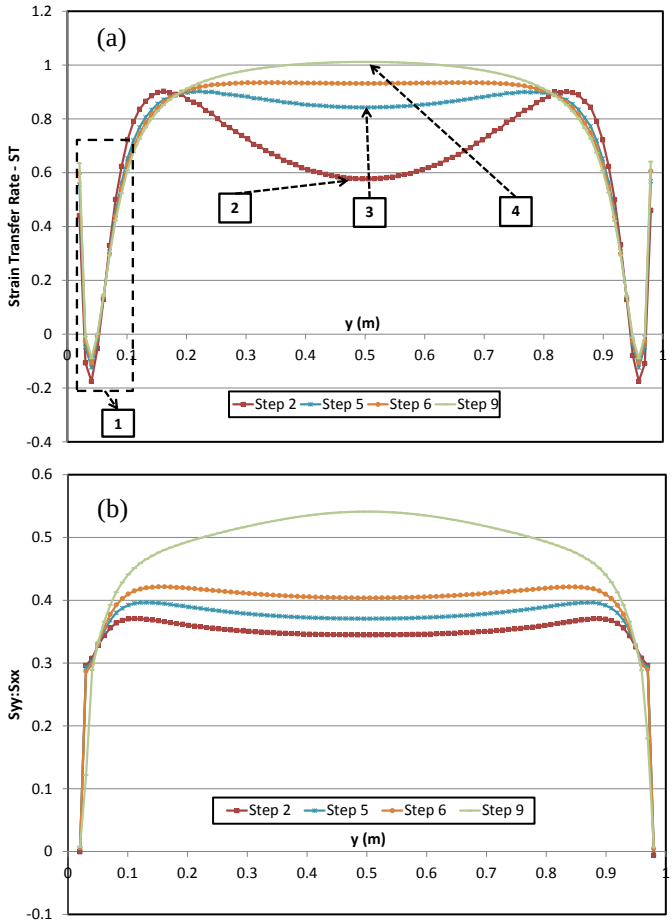

Fig. 6. a) Strain transfer rate at different step loadings for elastic behavior, b) vertical to horizontal stress ratio

Fig. 7 displays strain transfer rate, the same as Fig. 6a, except that the rock and grout can deform plastically. It can be seen that in general less strain is sensed in the fibre compared to Fig. 6a. At domain 1, the fibre registers more fluctuations and extension. It is also found that as loading increases, the fibre registers less strain from the middle of its length towards the ends such that over a short portion of its length it senses almost the same strain in rock. This seems to be the effect of grout going to yield.

Further to the grout stiffness case shown in Table 1, the borehole was also filled with grout with stiffness equal to and 1% of that of the rock. Fig. 8a is the strain transfer rate (*ST*) for grout to rock Young's modulus ratios (E_g:E_r) of 0.01, 0.2 (default grout), and 1 at two different loading steps. Apart from the end effects for all grout types, at step 2 (23 μm displacement loading), in the more compliant grout model (E_g:E_r=0.01) the strain in the fibre after reaching a peak of about 1 in the vicinity of the ends decreases rapidly toward the middle

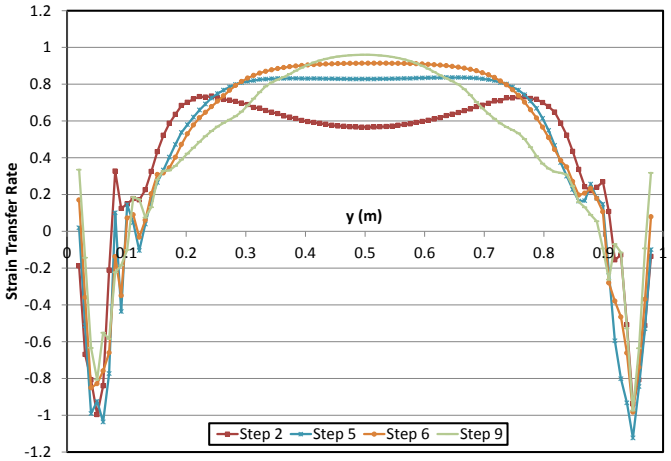

Fig. 7. Strain transfer rate at different step loadings considering plasticity

of the fibre with a sensing of just 26% of the rock strain, while with the default grout (E_g:E_r= 0.2), the fibre peaks at a lower strain (*ST* = 0.7) compared to the compliant one followed by a slight drop in the central section receiving near 60% of rock strain.

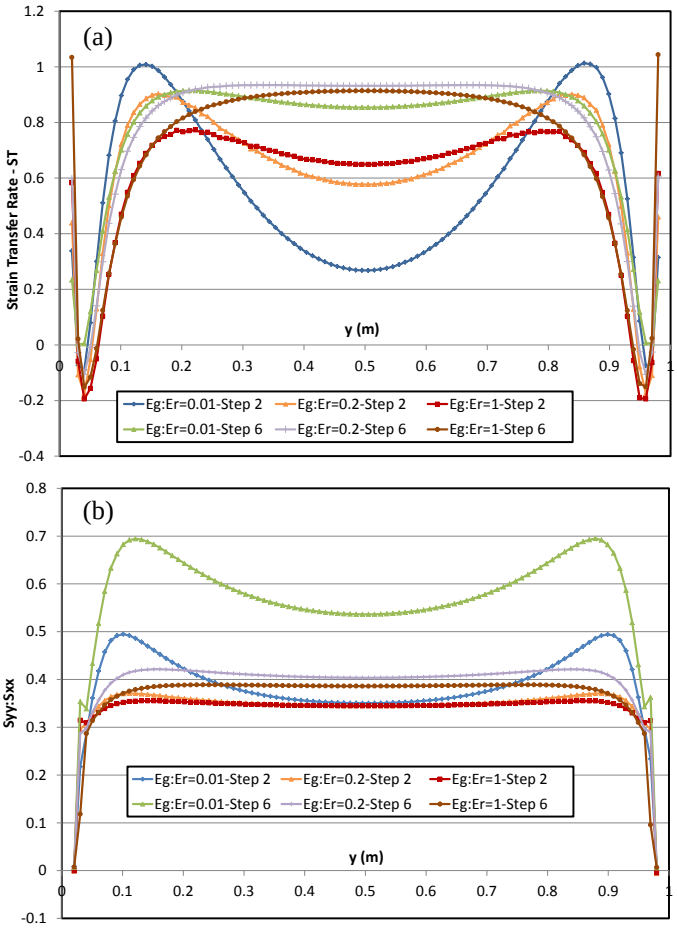

Fig. 8. a) Strain transfer rate and b) vertical to horizontal stress ratio in the fibre for various grout stiffnesses

In the case of the grout with the largest stiffness, the fibre registers the most uniform profile compared to the other models, sensing 65-75% of rock strain away from ends. The difference in profiles at this step between three grout types can be seen from Fig. 8b showing S_{yy}:S_{xx}. In general the ratio profile follows almost the same pattern as in Fig. 8a. Lower stiffness grout experiences more horizontal stress at both ends up to the points where the vertical stress becomes closer to horizontal (Fig8. b) causing the fibre to register a peak (Fig. 8a), while the grout with the highest stiffness shows more resistance to deformation in the x direction. At step 6 (115 μm displacement loading), the middle part of the fibre profile registers strains closer to the rock strain (maximum *ST* = 93%); but, from the ends toward the middle of the fibre, less strain is registered, especially at a higher grout stiffness (Fig. 8a). This is because S_{yy}:S_{xx} towards the middle of fibre increases with displacement loading (Fig. 8b). It can also be seen that as loading increases, the fibre covered by a stiffer grout shows slower deviation from the rock strain because of its higher bearing capacity. In addition, with softer grout, more of the length of the fibre registers closer strains to that of the rock. However, stiffer grout provides more resistance to deformation in the loading direction and since the grout and fibre are not loaded directly in the model, the stiffer grout generally transfers less strain to the fibre.

Another important parameter influencing strain transfer to the fibre is hole size or grout thickness. Fig. 9 gives the strain transfer rate at step 6 for various hole sizes.

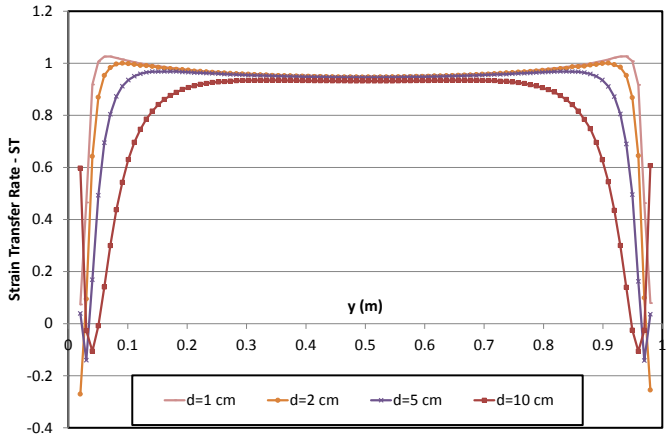

Fig. 9. Strain transfer rate for some borehole diameters at loading step 6

This shows that at the mid-point of the fibre, the strain is almost the same for all sizes, while as the size of borehole decreases to values closer to that of the fibre, the strain measured is closer to the rock strain over more of its length. It seems that a part of this difference is due to the boundary effect of thinner grout for a smaller hole on the fibre. If considering plasticity, the difference becomes more prominent.

It is also worth noting that the confinement condition has a minor effect in that the fibre will follow almost the same profile for all confining presses, but at later steps for larger confinements, as shown in Fig. 10 for the 6th loading step.

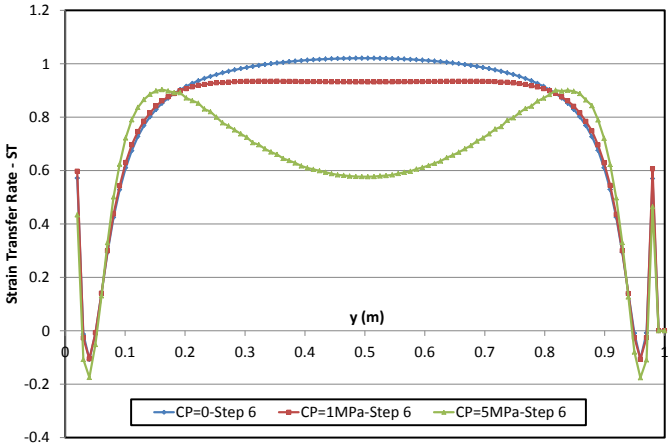

Fig. 10. Strain transfer rate for various confining pressures (CP)

4. DISCONTINUUM MODEL

The effect of fracture slippage on measured deformation in a grouted fiber is studied using the model shown in Fig. 4. Sensitivity to fracture angle and slippage amount has been evaluated. The strain transfer rate was examined for five fracture inclinations (θ) - 10°, 30°, 45°, 60°, and 75°, as shown in Fig. 11. The fracture is modeled by joint elements in the Phase2 finite element code with open nodes at the borehole wall and closed nodes at the extremities within the rock mass. The strain transfer rate displayed on Fig. 9 show that the fracture induces strain concentrations that locally result in ST>1. Fig. 11 also highlights the observation that the steeper the fracture, the more uniform is the strain transfer and the lower the strain concentrations that occur.

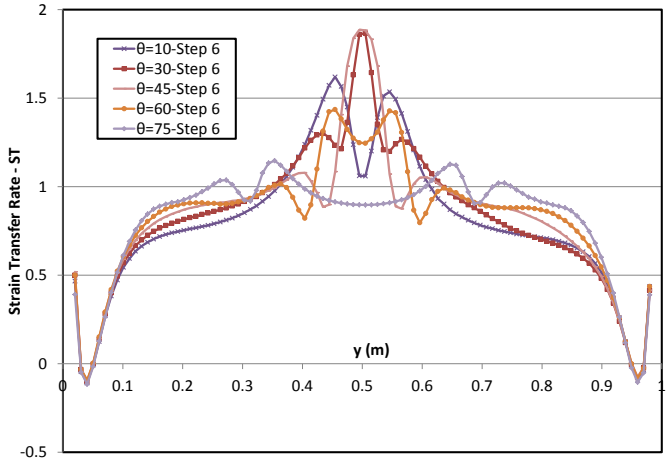

Fig. 11. Strain transfer rate for a single fracture crossing borehole at different inclinations

For inclinations ~<30° the modeling results show two clear peaks above and below the fracture, similar to the

conceptual representation of Fig. 3b. This response progressively disappears for steeper fractures: the two peaks become closer and closer to finally merge in the 45° case. Very steep fractures produce a response very similar to the homogeneous (no fracture) case.

Fig. 12 shows deformation bandwidth and horizontal offset experienced by the fibre as the fracture slips after 6th loading step. These values are calculated from the horizontal displacement profile along the fibre. From Fig. 12a, it can be seen that deformation bandwidth (w) (see Fig. 3) increases for steeper fractures. It also increases with loading to a peak, then stays at a constant value for higher loadings. Fig. 12b shows that offset (o in Fig. 3) for the 45° fracture is the greatest and it decreases as inclination diverges from 45°. From Fig. 12 is also shown that over 6 steps of loading the 45° fracture slips more than the other inclinations. This is in agreement with strain build-up at the middle of the fibre in Fig. 11, where the fracture crosses the borehole. Furthermore, at the location of the fracture, more strain is transferred to the fibre at higher loading steps with 30°, 45°, and 60° fractures (Fig. 11) which corresponds to more fracture shear displacement and horizontal offset for these inclinations, as shown in Fig. 12b.

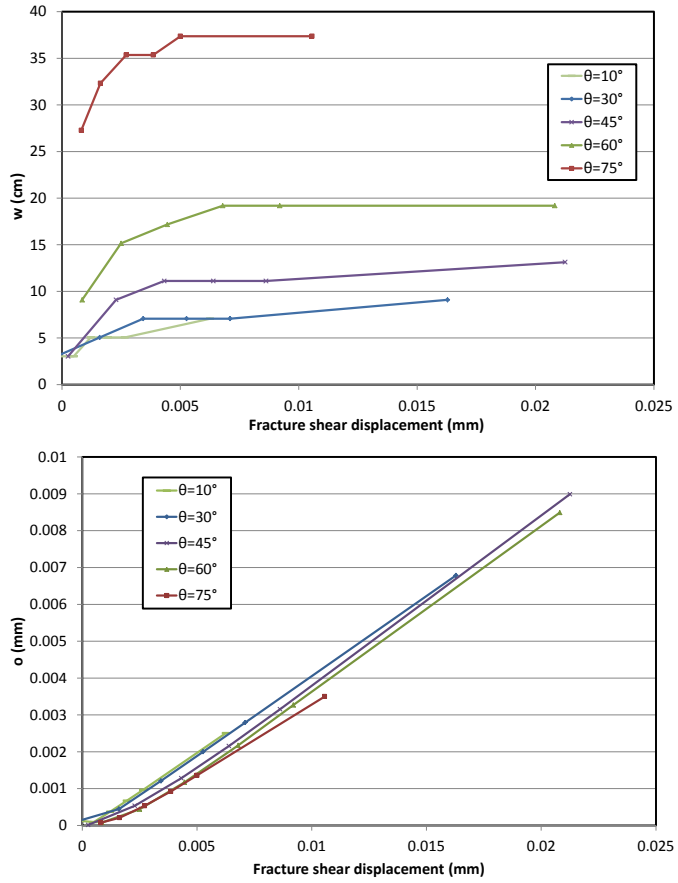

Fig. 12. a) Deformation bandwidth growth and b) fibre horizontal offset with fracture shear displacement

A sensitivity analysis of the grout stiffness effect on stain transfer is shown in Fig. 13. For this analysis the case of a 30° dipping fracture was considered. It can be seen that when grout is softer the strain is more localized near the trace of the fracture such that moving away from the trace of fracture, the strain is observed to decrease rapidly. Also, the fibre at each loading step becomes more strained, and with stiffer grout, the strain is more distributed.

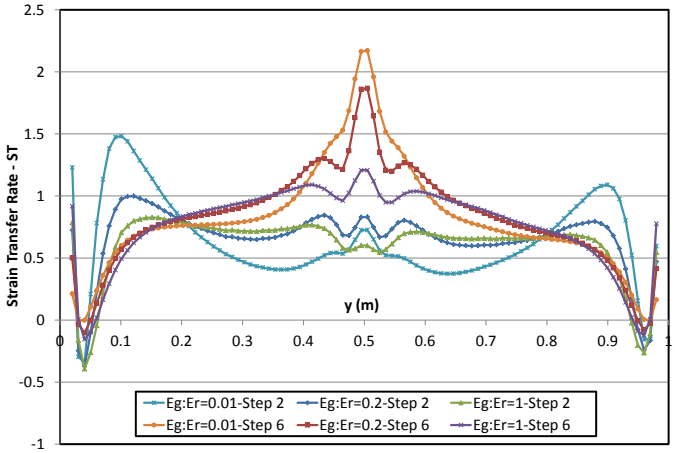

Fig. 13. Grout stiffness effect on strain transfer rate at the presence of a 30°-fracture

Now we consider two perpendicular joint sets with 30° and 150° inclinations to explore possible strain differences between the fibre and the rock. In this case, lateral boundaries are fixed to bring the model to convergence. Fig. 14 shows the strain transfer rate for this model for three different borehole grout stiffnesses. It is found that for any stiffness this configuration of joint sets causes the fibre to register much higher strain that that strain that occurs in the intact rock blocks. The fibre in all grouts shows strain fluctuating around an average especially at the mid-length of the fibre. It can be seen that although the fibre in the stiffest grout shows a shorter length of a uniform average strain profile, actually it measures a strain nearer to that of the rock (ST≈6), almost 15-30% closer than the other grouts (ST≈7-8). The strain profile changes as the joint sets inclination changes because of preferential joint slip.

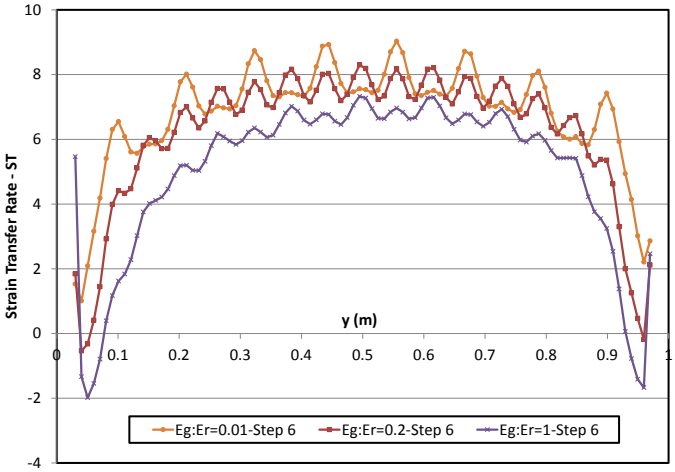

Fig. 14. Strain transfer rate for a rock block having 2 joint sets for three grout stiffnesses

5. CONCLUSION

Fully distributed fibre optic linear strain measurements are receiving more attention in underground mining. Borehole installation of optical fibre sensing cable was examined through a series of numerical models to understand how grout properties and borehole size influence the way the fibre register rock strain. Since grout at both ends of borehole lacks enough confinement, strains sensed by fibres in these sections should be cautiously used. In an assembly such as in this study, it was found that less stiff grout could measure a strain closer to what was occurring in the rock when sufficiently stressed, presenting almost the same effect as that of a smaller borehole.

The presence of a single fracture along which slip is permitted also changes the fibre strain profile, especially when the inclination is varied. It was illustrated that a 45° fracture causes the most strain concentration close to where the fracture trace passes through the borehole. Also, a fibre in a rock block containing two joint sets showed 6 to 8 times more strain than that occurring in the block, although this factor is clearly dependent the joint set inclinations.

ACKNOWLEDGEMENTS

This work is funded by an equipment grant from NSERC (National Sciences and Engineering Research Council of Canada), CEMI (Centre for Excellence in Mining Innovation) by the Ontario Ministry of Research and Innovation through the SUMIT (Smart Underground Monitoring and Integrated Technology) research program. Authors also would like to thank Rocscience Inc. for providing generous access to Phase2.

REFERENCES

1. Johnson, J.C., T. Brady, M. Larson, R. Langston, and H.Kirsten. 1999. Use of strain-gauged rock bolts to measure rock mass strain during drift development. In *Proceedings of the 37th U.S. Rock Mechanics Symposium, Vail, Colorado, June 6-9, 1999*, eds. B. Amadei et al, 497-502. Rotterdam: Balkema.
2. Ramsay, J. G. 1976. Displacement and strain. *Phil. Trans. R. Soc. Lond.* 283: 3-25.
3. Jaeger, J. C., N. G.W. Cook, and R. W. Zimmerman. 2007. *Fundamentals of Rock Mechanics*. 4th ed. Blackwell Publishing Ltd.